

RESEARCH ARTICLE

10.1002/2015WR018439

Key Points:

- A theory provides a quantitative basis for spatially lumped event-based rainfall-runoff prediction
- The SCS-CN method is extended with prethreshold and threshold-excess runoff mechanisms
- The theory provides spatially lumped models with an implicit spatial description of runoff

Correspondence to:

A. Porporato,
amilcare@duke.edu

Citation:

Bartlett, M. S., A. J. Parolari, J. J. McDonnell, and A. Porporato (2016), Beyond the SCS-CN method: A theoretical framework for spatially lumped rainfall-runoff response, *Water Resour. Res.*, 52, 4608–4627, doi:10.1002/2015WR018439.

Received 3 DEC 2015

Accepted 15 MAY 2016

Accepted article online 19 MAY 2016

Published online 18 JUN 2016

Beyond the SCS-CN method: A theoretical framework for spatially lumped rainfall-runoff response

M. S. Bartlett¹, A. J. Parolari¹, J. J. McDonnell^{2,3}, and A. Porporato¹

¹Department of Civil and Environmental Engineering, Duke University, Durham, North Carolina, USA, ²Global Institute for Water Security, University of Saskatchewan, Saskatoon, Canada, ³School of Geosciences, University of Aberdeen, Aberdeen, UK

Abstract Since its introduction in 1954, the Soil Conservation Service curve number (SCS-CN) method has become the standard tool, in practice, for estimating an event-based rainfall-runoff response. However, because of its empirical origins, the SCS-CN method is restricted to certain geographic regions and land use types. Moreover, it does not describe the spatial variability of runoff. To move beyond these limitations, we present a new theoretical framework for spatially lumped, event-based rainfall-runoff modeling. In this framework, we describe the spatially lumped runoff model as a point description of runoff that is upscaled to a watershed area based on probability distributions that are representative of watershed heterogeneities. The framework accommodates different runoff concepts and distributions of heterogeneities, and in doing so, it provides an implicit spatial description of runoff variability. Heterogeneity in storage capacity and soil moisture are the basis for upscaling a point runoff response and linking ecohydrological processes to runoff modeling. For the framework, we consider two different runoff responses for fractions of the watershed area: “prethreshold” and “threshold-excess” runoff. These occur before and after infiltration exceeds a storage capacity threshold. Our application of the framework results in a new model (called SCS-CN_x) that extends the SCS-CN method with the prethreshold and threshold-excess runoff mechanisms and an implicit spatial description of runoff. We show proof of concept in four forested watersheds and further that the resulting model may better represent geographic regions and site types that previously have been beyond the scope of the traditional SCS-CN method.

1. Introduction

Understanding and modeling the spatial variability of storm runoff at the watershed scale is fundamental to flood prediction, aquatic habitat location, soil erosion, and nonpoint source pollution [Sivapalan *et al.*, 1990; Naiman *et al.*, 1992; Cantón *et al.*, 2011; Carpenter *et al.*, 1998]. However, characterizing the spatial variability of runoff remains a major challenge because of nonlinearities inherent in runoff generation (e.g., thresholds) and the multiple hydrological states that result from the stochastic nature of rainfall and landscape heterogeneities [McDonnell *et al.*, 2007; Bartlett *et al.*, 2015; Ali *et al.*, 2013; Mirus *et al.*, 2011; Mirus and Loague, 2013]. Moreover, the spatial and temporal variability of runoff is perhaps the most poorly represented process in ecohydrological soil moisture models [e.g., Rodríguez-Iturbe and Porporato, 2004; Rigby and Porporato, 2006; Bartlett *et al.*, 2015]. Linking the ecohydrological controls of soil moisture to spatial runoff values is key to understanding nutrient, carbon, and other environmental fluxes.

Spatially distributed hydrologic models have been used to describe runoff variability through a detailed application of small-scale physics mapped explicitly to watershed heterogeneities [Ajami *et al.*, 2004; Beven, 2012; Ivanov *et al.*, 2004; Wigmosta *et al.*, 1994; Paniconi and Putti, 2015]. While such approaches provide reasonable results, fully distributed hydrological models are often complex with many parameters that require numerous data sets for calibration [Sivakumar *et al.*, 2013; Sivakumar and Singh, 2012; Semenova and Beven, 2015; Pathak *et al.*, 2015; Fatichi *et al.*, 2016]. For such reasons, hydrologists have resorted to spatially lumped or semidistributed models with fewer parameters [e.g., Fenicia *et al.*, 2011; Beven and Kirkby, 1979; Lindström *et al.*, 1997; Clark *et al.*, 2008].

Event-based models with spatially lumped variables are perhaps the least parametrically complex models. Within this genus of models, the Soil Conservation Service (now the Natural Resources Conservation Service)

curve number (SCS-CN) method is the most widely used in practice [Ponce and Hawkins, 1996; Beven, 2012, p. 228]. The SCS-CN method is embedded in a variety of models, e.g., soil erosion, flood control, and water quality [Hawkins, 2014; Garen and Moore, 2005; Ponce and Hawkins, 1996; Beven, 2012, p. 228]. The SCS-CN method predicts runoff from an expression for a rainfall-runoff curve that varies according to a single parameter called the curve number (CN). The dimensionless CN parameter describes the antecedent potential water retention of a watershed [Hawkins, 2014]. The method has become widely used because the CN value is tabulated for a variety of hydrologic conditions, land use types, and soil types. Consequently, these CN tables make it easy to transfer GIS data into a rainfall-runoff model based on the SCS-CN method [Beven, 2012, p. 229].

While useful in practice, the SCS-CN method is limited by its empirical origins [Beven, 2012; Ponce and Hawkins, 1996; Garen and Moore, 2005; Hawkins, 2014]. Developed from regional data mostly from agricultural sites in the Midwest region of the United States [Ponce and Hawkins, 1996], the SCS-CN method cannot be readily transferred to site types or regions outside the Midwest (although many studies around the world continue to do so). The SCS-CN method performs well in humid and subhumid regions for first-order and second-order watersheds, but it performs only fairly for rangeland sites and poorly for forested sites [Tedela et al., 2011; Ponce and Hawkins, 1996]. This poor performance likely reflects contrasting runoff mechanisms between agricultural and forested watersheds, the latter of which may be dominated by subsurface stormflow [Watson and Luxmoore, 1986]. The SCS-CN method also lacks a description of the spatial variability of runoff. Consequently, applications of the SCS-CN method have assumed a homogeneous watershed with a spatially uniform runoff process [Hawkins, 1982; Garen and Moore, 2005]. When SCS-CN runoff is applied uniformly over a watershed, significant errors can and do occur in the calculations of erosion, pollutant loading, and the source area of runoff [Garen and Moore, 2005]. With the exception of Steenhuis et al. [1995] who discussed the runoff source area, the theoretical derivations of the SCS-CN method [e.g., Yu, 1998; Schaake et al., 1996; Mishra and Singh, 1999] have focused almost exclusively on the average (lumped) runoff total without addressing the role of the spatial variability of antecedent soil moisture, multiple runoff mechanisms, runoff source areas, or the spatial variability of runoff over an area [Garen and Moore, 2005; Hawkins, 1982].

To move beyond the limitations of the SCS-CN method, we present a new theoretical framework that provides a quantitative basis for a spatially lumped event-based rainfall-runoff response. This framework has a probabilistic basis in a spatial distribution of water storage that is derived from distributions of spatially heterogeneous variables such as soil moisture. The framework uses the distribution of water storage to upscale a point description of the rainfall-runoff response to a watershed area, thus providing a probability density function (PDF) that characterizes the spatial variability of runoff and runoff type, where the spatial average is the "runoff curve," i.e., an expression for a rainfall-runoff relationship that is analogous to the SCS-CN method. This upscaling of soil moisture and rainfall-runoff patterns links ecohydrological processes to traditional SCS-CN runoff modeling. Following this framework, one may derive an event-based, spatially lumped model (e.g., SCS-CN method) based on a specific runoff response concept (i.e., mechanism of water delivery to the stream) and spatial distributions of watershed variables, e.g., rainfall, soil moisture, and storage capacity. Here we use this probabilistic storage (ProStor) framework to create a model (called SCS-CN_x) that extends the traditional SCS-CN method with a quantitative spatial characterization of runoff variability and a new representation of the runoff response via thresholds.

We start by reviewing the traditional SCS-CN method (section 2). In section 3, we outline the new theoretical ProStor framework for defining spatially lumped event-based rainfall-runoff models. Using the framework, we outline a new model that is specific to a runoff description based on thresholds (section 4). By assuming specific distributions of watershed variables, we then define a new event-based model, which we name the SCS-CN_x method (section 5). We discuss how the SCS-CN_x method has functionality that extends beyond the limitations of the traditional SCS-CN method (section 5). We compare the new SCS-CN_x method and the traditional SCS-CN method runoff curves to the data of four forested watersheds and then discuss the results (section 6).

2. The Traditional SCS-CN Method

First introduced in 1954 [Ponce and Hawkins, 1996; Rallison and Miller, 1982; USDA National Resources Conservation Service, 2004], the SCS-CN method is an empirical approach based on approximately 20 years of rainfall-runoff

data [Yuan *et al.*, 2001]. Most of these data were collected from small (less than 3 km²) experimental watersheds and plots that were mostly agricultural sites in the Midwestern United States [Ponce and Hawkins, 1996]. The general form of the SCS-CN method is

$$\bar{Q} = \begin{cases} 0 & \text{for } 0 \leq \bar{R} < \bar{I} \\ \frac{(\bar{R} - \bar{I})^2}{\bar{R} - \bar{I} + \bar{S}} & \bar{I} \leq \bar{R} < \infty, \end{cases} \quad (1)$$

where \bar{R} is the rainfall depth, \bar{Q} is the runoff depth, \bar{I} is the initial abstraction depth, and \bar{S} is the antecedent potential retention depth (all per unit area) [USDA National Resources Conservation Service, 2004]. Contrary to the typically SCS-CN method description, where \bar{S} is labeled as the maximum potential retention, we refer to \bar{S} as the antecedent potential retention to reflect that \bar{S} is a dynamic value that changes between storm events.

The initial abstraction, \bar{I} , represents an amount of rainfall that is retained in the watershed storage as interception, infiltration, and surface storage before runoff begins [Ponce and Hawkins, 1996]. By convention, the initial abstraction is a fraction of the antecedent potential retention, i.e.,

$$\bar{I} = \mu \bar{S}, \quad (2)$$

where μ is the initial abstraction ratio. The standard value is $\mu = 0.2$ but a value of $\mu = 0.05$ is considered to be more realistic [Ponce and Hawkins, 1996; Yuan *et al.*, 2001; USDA National Resources Conservation Service, 2004; Woodward *et al.*, 2002].

The antecedent potential retention \bar{S} is defined by the dimensionless CN parameter, i.e.,

$$\bar{S} = \frac{25,400}{\text{CN}} - 254, \quad (3)$$

where 25,400 and 254 are in units of millimeters. While the curve number theoretically may vary between 0 and 100, practical values are typically in the range of 40–98 [Ponce and Hawkins, 1996]. Tables provide a CN according to soil type, hydrologic condition, antecedent moisture condition, and land use [e.g., USDA National Resources Conservation Service, 2004].

3. Framework for Spatially Lumped, Event-Based Rainfall-Runoff Response

We assume that the watershed spatial heterogeneities can be implicitly represented by probability distributions. For simplicity, here we consider heterogeneous values of the soil moisture deficit, c , and water storage capacity, w ; however, in general, the framework could be expanded to include other heterogeneous variables that affect the water storage capacity, w , e.g., biotic variables such as root density or abiotic variables such as bedrock topography. Since any combination of variables results in a storage quantity, we call this a probabilistic storage (ProStor) framework. For a storm event, we assume each watershed point consists of a water storage capacity, w , with a soil moisture deficit, c , that is forced by a pulse of rainfall, R (Figure 1). Note that the soil moisture deficit, c , is a value between 0 and 1, and each point also may be considered in terms of the complementary relative soil moisture, i.e., $x = 1 - c$.

The rainfall pulse, R , represents a cumulative value for the storm duration, and thus the temporal dynamics of the storm are lumped. These lumped rainfall values are thus instantaneous inputs that increase soil moisture. It is reasonable to simplify storm events to lumped, instantaneous moisture inputs of rainfall because the moisture outputs, e.g., evapotranspiration, occur at a time scale that is much longer than the storm duration. For each storm event, the lumped rainfall values vary spatially over the watershed according to the PDF $p_R(R)$ and the unit area rainfall depth is the average $\bar{R} = \int_0^\infty R p_R(R) dR$.

The water storage capacity, w , is static in time and represents the maximum depth of soil water that may be detained at a point. Before rainfall increases the stored soil water depth to the water storage capacity, i.e., $x < 1$, certain watershed points may produce prethreshold runoff with a magnitude that varies with x (Figure 1). Otherwise, when rainfall increases the soil water depth to capacity, i.e., $x = 1$, rainfall spills as threshold-excess runoff (Figure 1). The storage capacity, w , may vary spatially because of the plant rooting

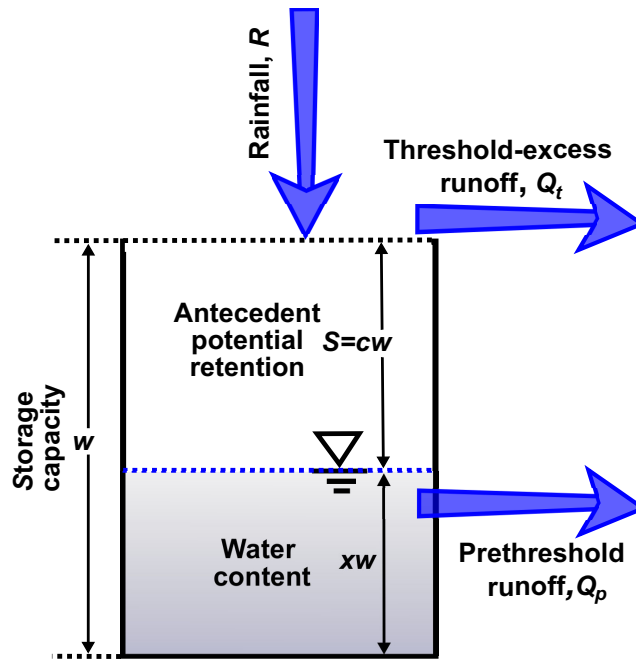


Figure 1. Schematic of a watershed point consisting of the storage capacity, w , where the antecedent potential retention, $S=cw$, indicates the spare depth of storage that depends on the antecedent soil moisture deficit, c . Rainfall, R , causes threshold-excess runoff, Q_t , when the water content equals the storage capacity, but before the storage capacity threshold of some watershed points, rainfall also initiates “prethreshold” runoff, Q_p .

watershed, i.e., $\bar{c} = 1$, will detain rainfall. Watershed saturation is often described in terms of the complementary average relative soil moisture $\bar{x} = 1 - \bar{c}$. For a list of variables and parameters, see Table 1.

3.1. Runoff Variability PDF and Average Runoff

For each storm event, the spatial variability of the system can be represented by a joint PDF. Here we assume the joint PDF is of runoff, Q , and R , c , and w , i.e.,

$$p_{QRcw}(Q, R, c, w) = p_{Q|RCw}(Q|R, c, w)p_{RCw}(R, c, w). \quad (4)$$

More general forms of this PDF may include additional variables such as rainfall intensity or soil porosity. In an event-based representation, the rainfall-runoff response at a watershed point is assumed to be a deterministic function of variables from the joint PDF, i.e.,

$$Q = Q(R, c, w), \quad (5)$$

| Symbol | Description |
|---------|--|
| R | Storm event rainfall depth at a point |
| w | Water storage capacity depth at a point |
| c | Antecedent soil moisture deficit at a point, $(1-x)$ |
| x | Antecedent soil moisture at a point, $(1-c)$ |
| S | Antecedent potential retention at a point, $S=cw$ |
| μ | Initial abstraction ratio; see equation (2) |
| F_t | Fraction of watershed with threshold-excess runoff |
| Q | Storm event runoff depth at a point |
| Q_p | Prethreshold runoff depth at a point over $(1-F_t)$ |
| Q_t | Threshold-excess runoff depth at a point over F_t |
| β | Fraction of watershed with nonzero prethreshold runoff |
| P_i | Prethreshold runoff index, $P_i = \beta(1-\bar{c})$ |

^aVariables in the text with an overline bar indicate a spatial average (unit area) depth value, e.g., for the point rainfall depth, R , the average (unit area) value is denoted by \bar{R} . All values have dimensions of length except c , x , μ , β , P_i , and F_t , which are dimensionless.

depth, surface topography, bedrock topography, bedrock permeability, or the depth to the groundwater table [e.g., Hopp and McDonnell, 2009]. The spatial variability of w is given by the PDF $p_w(w)$, and the unit area storage capacity of the watershed is the average $\bar{w} = \int_0^{w_{\max}} wp_w(w)dw$, where w_{\max} is the largest point storage capacity in the watershed.

The antecedent soil moisture deficit, c , represents the fraction of w that is empty prior to the storm event (Figure 1). Before the storm, the empty spare depth of storage is given by the antecedent potential retention, $S=cw$ (Figure 1), where $S_{\max} = w_{\max} c_{\max}$ is the greatest point value found in the watershed area. The spatial variability of c is characterized by the PDF $p_c(c)$, and the average $\bar{c} = \int_0^1 cp_c(c)dc$ indicates the global deficit in watershed storage that may detain rainfall. A fully saturated watershed where no water infiltrates, i.e., $\bar{c} = 0$, will detain zero rainfall, whereas a completely dry

watershed, i.e., $\bar{c} = 1$, will detain rainfall. Watershed saturation is often described in terms of the complementary average relative soil moisture $\bar{x} = 1 - \bar{c}$. For a list of variables and parameters, see Table 1.

and in general, this function could be expanded to additional variables if they are included in the joint PDF of equation (4). Because of the deterministic rainfall-runoff response, the PDF of Q conditional on R , c , and w is a point mass of probability,

$$p_{Q|RCw}(Q|R, c, w) = \delta(Q(R, c, w) - Q), \quad (6)$$

where $\delta(\cdot)$ is the Dirac delta function. In contrast to a continuous probability distribution, a point mass indicates that only one value of Q occurs for a

given R , c , and w . Thus, equation (6) states that with probability of 1, Q assumes the value of the RHS of equation (5).

For each storm event, the joint PDF $p_{RCW}(R, c, w)$ represents the spatial variation of R , c , and w over the watershed area. In terms of R and c , the PDF $p_{RCW}(R, c, w)$ may vary for each storm, however, in terms of w , the PDF is static in time. Here we reasonably assume that rainfall, R , is statistically independent from both the antecedent soil moisture deficit, c , and storage capacity, w , so equation (4) becomes

$$p_{QRCW}(Q, R, c, w) = \delta(Q(R, c, w) - Q) p_R(R) p_{cw}(c, w). \quad (7)$$

The runoff PDF is the marginal PDF of $p_{QRCW}(Q, R, c, w)$, i.e.,

$$p_Q(Q) = \int_0^{w_{\max}} \int_0^1 \int_0^\infty p_{QRCW}(Q, R, c, w) dR dc dw. \quad (8)$$

In equation (8), integration over the delta function, which results from equation (7), is performed using the property presented in Appendix E.

The cumulative distribution function (CDF), $P_Q(Q)$, is equal to the fraction of watershed area, F , where runoff is less than or equal to Q . Conversely, the inverse CDF (quantile function),

$$Q = P_Q^{-1}(F), \quad (9)$$

gives the maximum value of runoff, Q , found within the fraction of watershed area, F .

The average runoff for the watershed area is

$$\bar{Q} = \int_0^\infty Q p_Q(Q) dQ, \quad (10)$$

which is also the runoff depth on a unit area basis. Equation (10) provides what is typically referred to as the "runoff curve."

3.2. The PDF for the Antecedent Soil Moisture Deficit and Storage Capacity

The joint PDF of c and w is given by

$$p_{cw}(c, w) = p_{c|w}(c|w) p_w(w), \quad (11)$$

where $p_{c|w}(c|w)$ is the conditional PDF for the distribution of the antecedent soil moisture deficit. The PDF $p_{c|w}(c|w)$ arises from local effects, e.g., evapotranspiration and soil type, and the nonlocal effect of lateral moisture redistribution.

In perhaps the simplest approach, we approximate $p_{cw}(c, w)$ with the PDF

$$\hat{p}_{cw}(c, w; \bar{c}) = \hat{p}_{c|w}(c|w; \bar{c}) p_w(w), \quad (12)$$

where $p_{c|w}(c|w)$ is now represented by the new form $\hat{p}_{c|w}(c|w; \bar{c})$ where the parameters (e.g., shape and location) are defined in terms of \bar{c} . We assume the PDF $\hat{p}_{c|w}(c|w; \bar{c})$ is unique to the physical characteristics of a watershed, e.g., bedrock and surface topography and preferential flow arrangements. Through these characteristics, changes in \bar{c} directly correspond to changes in the strength of the local and nonlocal effects that alter the distribution of the antecedent soil moisture deficit. [Western *et al.*, 1999, 2004; Yeakley *et al.*, 1998]. The only restriction on equation (12) is that it must satisfy the self-consistent condition

$$\bar{c} = \int_0^1 \int_0^{w_{\max}} c \hat{p}_{c|w}(c|w; \bar{c}) p_w(w) dw dc. \quad (13)$$

The PDF $\hat{p}_{c|w}(c|w; \bar{c})$ may incorporate complex relationships between the spatial distribution of the antecedent soil moisture deficit and the watershed average \bar{c} . For example, the functional form of the PDF could account for multiple modes in the soil moisture deficit distribution under different average conditions [e.g., Ryu and Famiglietti, 2005], and the functional dependence of PDF parameters on \bar{c} could model the hysteresis in the variability of the soil moisture deficit [e.g., Ivanov *et al.*, 2010; Fatichi *et al.*, 2015].

The most basic assumption for $\hat{p}_{c|w}(c|w; \bar{c})$ is that each point value of c is equal to the watershed average \bar{c} . For this assumption, $\hat{p}_{c|w}(c|w; \bar{c})$ becomes the independent distribution $\hat{p}_c(c; \bar{c}) = \delta(c - \bar{c})$, where the Dirac

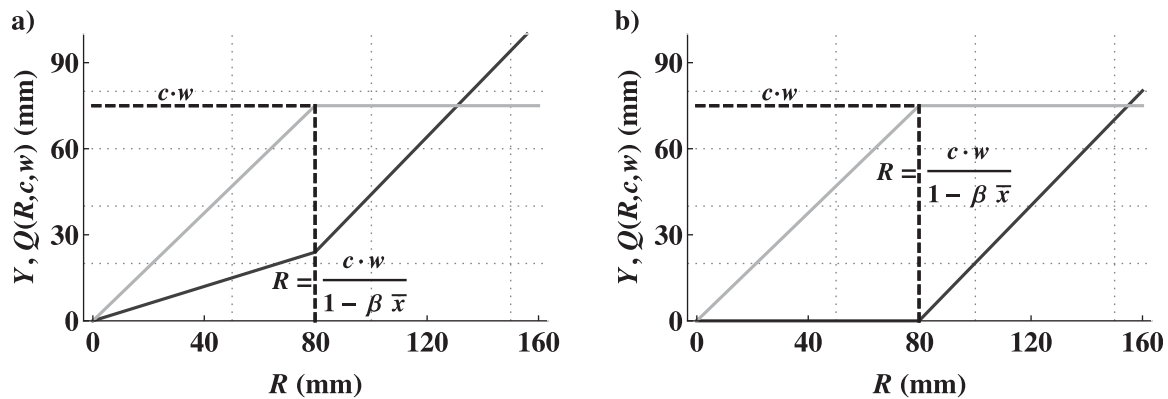


Figure 2. The rainfall-runoff response at a point (black line) for (a) $Q_1(R, c, w)$ of equation (14) for the fraction of area β and (b) $Q_2(R, c, w)$ of equation (15) for the fraction of area $1 - \beta$. In both cases, the threshold-excess occurs when the rainfall amount exceeds $R = (c \cdot w) / (1 - \beta \bar{x})$ for which infiltration at a point (gray line), $Y = R - \beta Q_1(R, c, w) - (1 - \beta) Q_2(R, c, w)$, equals the antecedent potential retention, $c \cdot w$. Cases are shown for $\bar{x} = 0.3$.

delta function $\delta(\cdot)$ indicates that c is equal to \bar{c} with probability 1. This basic case will be discussed in section 5, and it may be representative of the small experimental watersheds that are the basis of the SCS-CN method.

4. Rainfall-Runoff Model

Following the ProStor framework described in section 3, we now develop an event-based model by assuming specific point rainfall-runoff responses for equation (5). The resulting model is general to any assumptions for $p_R(R)$ and $\hat{p}_{cw}(c, w; \bar{c})$.

4.1. Point Rainfall-Runoff Response

The watershed is conceptualized as two areas, each with a unique description of the rainfall-runoff response based on a storage capacity threshold. Over the fraction of area β , runoff is assumed to occur both before and after infiltration exceeds the storage capacity threshold (Figure 2a, black line), i.e.,

$$Q_1(R, c, w) = \begin{cases} R\bar{x} & \text{for } 0 \leq R < \frac{c \cdot w}{1 - \beta \bar{x}} \\ R - c \cdot w \frac{1 - \bar{x}}{1 - \beta \bar{x}} & \frac{c \cdot w}{1 - \beta \bar{x}} \leq R < \infty. \end{cases} \quad (14)$$

The “prethreshold” runoff, $R\bar{x}$, is controlled by the watershed wetness, represented by the average antecedent soil moisture \bar{x} . As \bar{x} increases, the runoff flow increases as larger soil pores fill and connect to thus expand the flow network capacity to transmit prethreshold runoff to the stream [Sidle et al., 2000; Kim et al., 2005; Lin, 2012].

Over the complementary fraction of watershed area, $1 - \beta$, runoff is assumed to occur only when infiltration exceeds the storage capacity threshold (Figure 2b, black line), i.e.,

$$Q_2(R, c, w) = \begin{cases} 0 & \text{for } 0 \leq R < \frac{c \cdot w}{1 - \beta \bar{x}} \\ R - \frac{c \cdot w}{1 - \beta \bar{x}} & \frac{c \cdot w}{1 - \beta \bar{x}} \leq R < \infty. \end{cases} \quad (15)$$

In both equations (14) and (15), the rainfall amount for threshold-excess runoff, $\frac{c \cdot w}{1 - \beta \bar{x}}$, accounts for lateral moisture redistribution by assuming infiltration at each point is equal to rainfall minus the spatial average of prethreshold runoff over the watershed, i.e., $R - \beta R \bar{x}$. When $R = \frac{c \cdot w}{1 - \beta \bar{x}}$, the infiltration amount, $R - \beta R \bar{x}$, equals the antecedent potential retention, $c \cdot w$. Because of this lateral moisture redistribution from the fraction of area $1 - \beta$ to the fraction of area β , the soil moisture deficit is the same for points in both areas that are adjacent to each other.

4.2. Lumped Rainfall-Runoff Response

The previously defined rainfall-runoff responses are substituted into equation (7) to find the corresponding PDFs $p_{Q_1,RCW}(Q, R, c, w)$ and $p_{Q_2,RCW}(Q, R, c, w)$. Because each PDF represents a mutually exclusive area, the PDF for the entire watershed, $p_{QRcW}(Q, R, c, w)$, is equal to the weighted sum $\beta p_{Q_1,RCW}(Q, R, c, w) + (1-\beta)p_{Q_2,RCW}(Q, R, c, w)$, i.e.,

$$p_{QRcW}(Q, R, c, w) = \begin{cases} \beta \delta(R\bar{x} - Q) p_R(R) \hat{p}_{cW}(c, w; \bar{c}) & \text{for } 0 \leq R < \frac{cW}{1-\beta\bar{x}} \\ + (1-\beta) \delta(Q) p_R(R) \hat{p}_{cW}(c, w; \bar{c}) & \\ \beta \delta\left(R - cW \frac{1-\bar{x}}{1-\beta\bar{x}} - Q\right) p_R(R) \hat{p}_{cW}(c, w; \bar{c}) & \frac{cW}{1-\beta\bar{x}} \leq R < \infty. \\ + (1-\beta) \delta\left(R - \frac{cW}{1-\beta\bar{x}} - Q\right) p_R(R) \hat{p}_{cW}(c, w; \bar{c}) & \end{cases} \quad (16)$$

The terms for $0 \leq R < \frac{cW}{1-\beta\bar{x}}$ describe the watershed region of prethreshold runoff production where the delta function, $\delta(Q)$, represents the discrete atom of probability for zero runoff. The terms for $\frac{cW}{1-\beta\bar{x}} \leq R < \infty$ describe the region of threshold-excess runoff.

The fraction of watershed area that produces threshold-excess runoff is found by integrating $p_R(R) \hat{p}_{cW}(c, w; \bar{c})$ over the range $\frac{cW}{1-\beta\bar{x}} \leq R < \infty$, i.e.,

$$F_t = \int_0^{W_{max}} \int_0^1 \int_{\frac{cW}{1-\beta\bar{x}}}^{\infty} p_R(R) \hat{p}_{cW}(c, w; \bar{c}) dR dc dw. \quad (17)$$

For the complementary fraction of watershed area, $1-F_t$, prethreshold runoff occurs over the fraction of area $(1-F_t)\beta$ but is zero over the fraction of area $(1-F_t)(1-\beta)$. Note that the total fraction of the watershed producing runoff is equal to $F_t + (1-F_t)\beta$.

The PDF of runoff, $p_Q(Q)$, is the weighted sum of the PDFs for prethreshold runoff, $p_{Q_p}(Q)$, and threshold-excess runoff, $p_{Q_t}(Q)$, i.e.,

$$p_Q(Q) = (1-F_t)p_{Q_p}(Q) + F_t p_{Q_t}(Q). \quad (18)$$

The fraction of area $1-F_t$ is the normalization constant for the prethreshold runoff PDF, i.e.,

$$p_{Q_p}(Q) = (1-\beta)\delta(Q) + \frac{\beta}{1-F_t} \left(\frac{1}{\bar{x}} p_R\left(\frac{Q}{\bar{x}}\right) \int_0^{W_{max}} \int_{\frac{Q}{\bar{x}} \frac{(1-\beta\bar{x})}{x}}^1 \hat{p}_{cW}(c, w; \bar{c}) dc dw \right), \quad (19)$$

where $0 < Q < \left(\frac{S_{max}\bar{x}}{1-\beta\bar{x}}\right)$. In equation (19), the delta function represents an atom of probability for zero runoff over the fraction of area $1-\beta$, while the continuous PDF in the second term represents prethreshold runoff variability over the fraction of area β (see Figure 3). Likewise, the fraction of area F_t is the normalization constant for the threshold-excess runoff PDF, i.e.,

$$p_{Q_t}(Q) = \frac{1}{F_t} \left((1-\beta) \int_0^{W_{max}} \int_0^1 p_R\left(Q + \frac{cW}{1-\beta\bar{x}}\right) \hat{p}_{cW}(c, w; \bar{c}) dc dw \right. \\ \left. + \beta \int_0^{W_{max}} \int_0^1 p_R\left(Q + cW \frac{1-\bar{x}}{1-\beta\bar{x}}\right) \hat{p}_{cW}(c, w; \bar{c}) dc dw, \right. \\ \left. - \beta \int_0^{W_{max}} \int_{\frac{Q}{\bar{x}} \frac{(1-\beta\bar{x})}{x}}^1 p_R\left(Q + cW \frac{1-\bar{x}}{1-\beta\bar{x}}\right) \hat{p}_{cW}(c, w; \bar{c}) dc dw \right), \quad (20)$$

where $0 \leq Q < \infty$. The first term represents the variability of threshold-excess runoff for the fraction of area $1-\beta$, while the second and third terms collectively represent the fraction of area β (see Figure 3). While the first and second terms are for runoff between $0 \leq Q < \infty$, the third term is for runoff between $0 \leq Q < \frac{S_{max}\bar{x}}{1-\beta\bar{x}}$.

The average unit area runoff is the weighted sum of the average prethreshold and threshold-excess runoff, i.e.,

$$\bar{Q} = (1 - F_t) \int_0^{\frac{S_{\max} \bar{x}}{1 - \beta \bar{x}}} Q p_{Q_p}(Q) dQ + F_t \int_0^{\infty} Q p_{Q_t}(Q) dQ, \quad (21)$$

where for $\beta = 0$, the first term is zero because $p_{Q_p}(Q) = \delta(Q)$.

5. The Extended SCS-CN Method (SCS-CN_x)

Starting from the model expressions of the previous section, we derive an extended SCS-CN method (SCS-CN_x) by assuming specific distributions of $p_R(R)$ and $\hat{p}(c, w; \bar{c})$. We assume the spatial distribution of rainfall is exponential, i.e.,

$$p_R(R) = \frac{1}{\bar{R}} e^{-R/\bar{R}}, \quad (22)$$

and past studies have used the same PDF form to derive the SCS-CN method [Yu, 1998; Schaake et al., 1996]. The exponential distribution has been used to describe rainfall variability in the grid cells of climate models and large-scale hydrologic models [Thomas and Henderson-Sellers, 1991; Liang et al., 1996; Tang et al., 2007; Sivapalan et al., 1997; Shuttleworth, 1988; Arnell, 2014, p. 279] and also has been shown to be suitable for representing the rainfall variability over small watersheds of about 40 km² [Schaake et al., 1996].

In addition, we consider the limiting case of spatially homogeneous antecedent soil moisture and assume $\hat{p}_{cw}(c, w; \bar{c})$ is represented by

$$\hat{p}_{cw}(c, w; \bar{c}) = \hat{p}_c(c; \bar{c}) p_w(w) = \delta(c - \bar{c}) \frac{1}{\bar{w}} e^{-w/\bar{w}}, \quad (23)$$

where $0 \leq w < \infty$. The independent soil moisture deficit PDF, $\hat{p}_c(c; \bar{c})$, is the point mass of probability $\delta(c - \bar{c})$. This point mass specifies zero spatial variability in the soil moisture deficit because it indicates that each point in the watershed experiences the average watershed soil moisture deficit, i.e., $c = \bar{c}$. The PDF $\delta(c - \bar{c})$ may roughly represent the small experimental watersheds (<3 km²) that are the basis of the SCS-CN method because smaller watersheds typically show less spatial variability in the soil moisture deficit [Famiglietti et al., 2008; Rodriguez-Iturbe et al., 1995]. The PDF $\delta(c - \bar{c})$ also may approximate watersheds where vegetation homogenizes soil moisture and acts to destroy spatial variability [Ivanov et al., 2010; Teuling and Troch, 2005]. The PDF $p_w(w)$ is typically unknown for a watershed, and the exponential distribution of equation (23) represents the most conservative probabilistic model according to the theory of maximum entropy [e.g., Jaynes and Bretthorst, 2003].

5.1. Fraction of Area With Threshold-Excess Runoff

Using these assumptions for $p_R(R)$ and $\hat{p}_{cw}(c, w; \bar{c})$, the fraction of area with threshold-excess runoff by the end of the storm event is

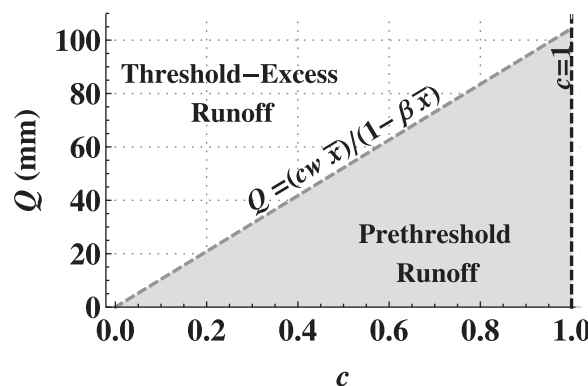


Figure 3. For the terms of equations (19) and (20) that represent the fraction of area β , the threshold-excess region of integration (white) and the prethreshold region of integration (gray) for $\beta = 0.35$, $\bar{x} = 0.8$, and $w_{\max} = 200$ mm. The boundary between the two regions (dashed line) is given by the runoff response of equation (14) when $R = (cw)/(1 - \beta \bar{x})$.

$$F_t = \frac{\bar{R}(1 - \beta(1 - \bar{c}))}{\bar{c}\bar{w} + \bar{R}(1 - \beta(1 - \bar{c}))}, \quad (24)$$

based on equation (17) where \bar{c} and β are parameters characterizing antecedent conditions. This fraction of area varies with the average rainfall amount: as \bar{R} approaches infinity, F_t approaches 1, and conversely, when \bar{R} is 0, F_t is also 0. Increasing the fraction of area β decreases the fraction of area with threshold-excess runoff (Figure 4a). F_t also decreases when \bar{c} increases (Figure 4b). The F_t of equation (24) is smaller than the form derived by Steenhuis et al. [1995]; see Figure 4a and Appendix A.

5.2. Runoff PDF

Following equation (18), the runoff PDF, i.e.,

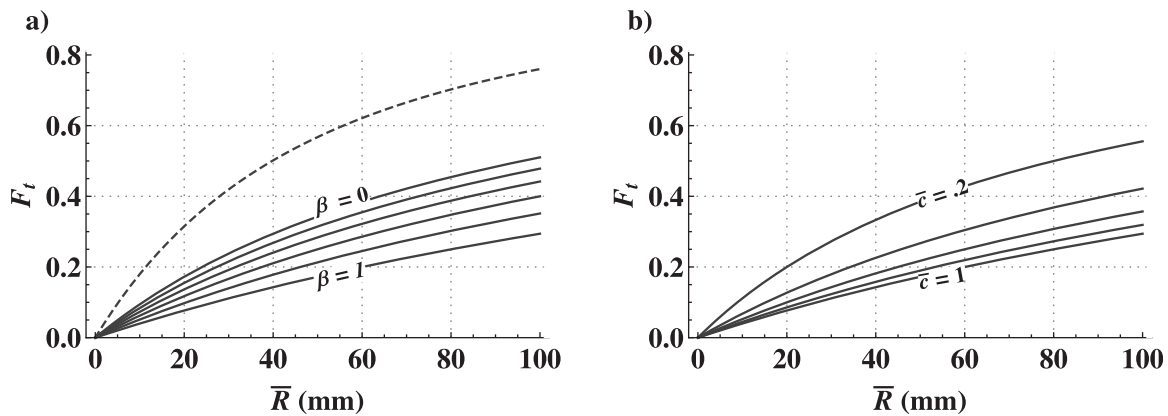


Figure 4. Equation (24) fraction of area with threshold-excess runoff, F_t , as a function of the average rainfall, \bar{R} , when $\bar{w}=240$ mm for (a) different fractions of the prethreshold area, β , when $\bar{c}=0.4$, and (b) different average antecedent soil moisture deficits, \bar{c} , when $\beta=0.5$. For the SCS-CN method of equation (27) when $\beta=0$, the F_t suggested by Steenhuis et al. [1995] (dashed line) is greater than the F_t of equation (24) when $\beta=0$ (see Appendix A).

$$p_Q(Q) = (1-\beta)(1-F_t)\delta(Q) + \beta \frac{e^{-\frac{Q}{(1-F_t)(1-\bar{c})\bar{R}}}}{R(1-\bar{c})} + (1-\beta)F_t \frac{1}{\bar{R}} e^{-\frac{Q}{\bar{R}}} + \beta e^{-\frac{Q}{\bar{R}}}(1-(1-\bar{c})\beta) \frac{1 - e^{-\frac{Q^2 \bar{w} + \bar{R}(1-(1-\bar{c})\beta)}{c\bar{w}(1-\bar{c})\bar{R}}}}{c^2 \bar{w} + \bar{R}(1-(1-\bar{c})\beta)}, \tag{25}$$

is the weighted sum of respective PDFs for prethreshold and threshold-excess runoff (see Appendix B). The first and second terms of equation (25) represent the variability of prethreshold runoff, while the third and fourth terms collectively represent the variability of threshold-excess runoff. The prethreshold runoff contributes to the bulk of the probability density for smaller runoff values and includes an atom for the discrete probability of zero runoff (Figure 5, dashed line and black bar). For larger runoff values, the bulk of the probability density is attributed to threshold-excess runoff (Figure 5, gray line).

5.3. Average Runoff (the Runoff Curve)

The main result of the SCS-CN_x method is the average unit area runoff,

$$\bar{Q} = \frac{\bar{R}^2 + (\bar{S} - \bar{R})\bar{R}P_i}{\bar{S} + \bar{R}(1 - P_i)}, \tag{26}$$

where $\bar{Q} > 0$ for any \bar{R} , $\bar{S} = \bar{c}\bar{w}$ is the average antecedent potential retention, and $P_i = \beta(1-\bar{c})$ is the prethreshold runoff index. For a watershed of area A , the total runoff volume is $A\bar{Q}$. Following equation (21), equation (26) is the weighted sum of the average prethreshold runoff, \bar{Q}_p , and the average threshold-excess runoff, \bar{Q}_t (see Appendix B). As P_i increases, prethreshold runoff significantly increases the total runoff for small rainfall events (Figure 6). However, for larger rainfall events, the threshold-excess runoff accounts for the majority of the total runoff (Figure 6). For both small and large storms, runoff increases significantly when \bar{c} is reduced (Figure 6).

When $\beta=0$ ($P_i=0$), equation (26) simplifies to the traditional SCS-CN method curve (equation (1)) without the initial abstraction term, i.e.,

$$\bar{Q} = \bar{R} F_t = \frac{\bar{R}^2}{\bar{S} + \bar{R}}. \tag{27}$$

Equation (27) is simply the product of the average rainfall, \bar{R} , and the fraction of area

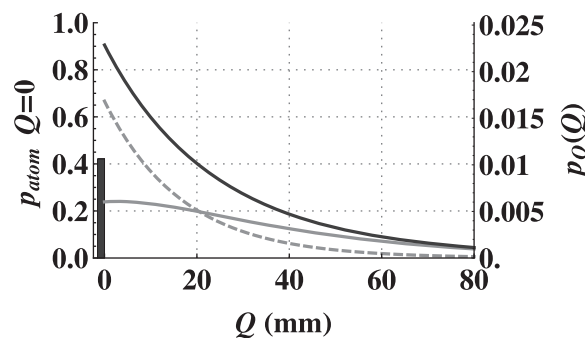


Figure 5. The spatial runoff PDF of equation (25) consists of a continuous distribution (black line) and an atom of probability for the discrete probability of zero runoff (black bar). The PDF is the weighted prethreshold runoff PDF of equation (B4) with the atom of probability for zero runoff (dashed line and black bar for $P(Q=0)=0.42$, i.e., $(1-F_t)p_{Q_0}(Q)$, plus the weighted threshold-excess runoff PDF (gray line) of equation (B5), i.e., $F_t p_{Q_t}(Q)$. PDFs shown for values of $\bar{w}=240$ mm, $\bar{c}=0.2$, $\beta=0.4$, and $\bar{R}=30$ mm.

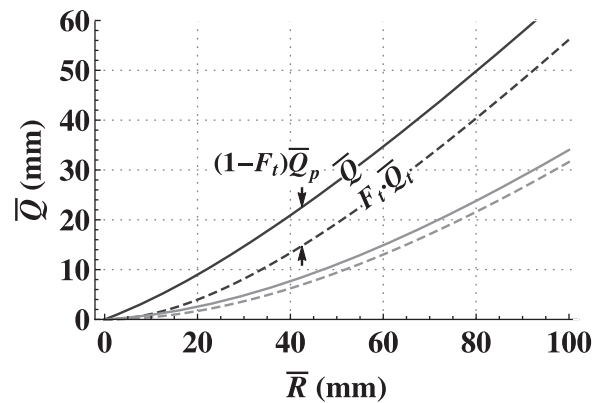


Figure 6. The average runoff, \bar{Q} (solid lines) of equation (26), versus average rainfall, \bar{R} . The average runoff is the total of the weighted average threshold-excess runoff, $F_t\bar{Q}_t$ (dashed lines) of equation (B7), and the weighted average prethreshold runoff, $(1-F_t)\bar{Q}_p$ of equation (B6). Cases shown for an average antecedent soil moisture deficits of $\bar{c}=0.3$ (black lines) and $\bar{c}=0.9$ (gray lines) where in both cases $\beta=0.5$ and $\bar{w}=240$ mm.

threshold-excess runoff PDFs. The quantile function equals the maximum value of runoff found within a fraction of the watershed area, F . For F from 0 to 1, the quantile functions show the variability of the runoff depth over the watershed. Here we consider two watershed areas: (1) the fraction of area between 0 and F_t where threshold-excess runoff occurs and (2) the fraction of area between F_t and 1 where prethreshold runoff occurs (Figure 7).

For the fraction of area with threshold-excess runoff, i.e., $0 \leq F \leq F_t$, the quantile function,

$$Q_t = P_{Q_t}^{-1}\left(\frac{F}{F_t}\right), \quad (28)$$

is given by the inverse of equation (C3) CDF in Appendix C. For this fraction of area between 0 and F_t , Figure 7 shows the variability of the threshold-excess runoff depth. For the fraction of area with prethreshold runoff, i.e., $F_t < F \leq 1$, the quantile function,

$$Q_p = P_{Q_p}^{-1}\left(\frac{F-F_t}{1-F_t}\right), \quad (29)$$

is given by equation (C4) in Appendix C. The prethreshold runoff is zero over the fraction of area between F_t and $F_t + (1-F_t)(1-\beta)$, but the prethreshold runoff is a variable depth over the fraction of area between $F_t + (1-F_t)(1-\beta)$ and 1 (Figure 7). The overall profile of runoff variability for the watershed (Figure 7) may be viewed as the combination of the threshold-excess runoff profile of equation (28) over F_t and the prethreshold runoff profile of equation (29) over $1-F_t$ (Figure 7).

For a fraction of the watershed, F , the average (unit area) runoff is the area between 0 and F under the profile curves of equations (28) and (29) (see Figure 7). As the fraction, F , increases from 0 to 1, the cumulative area under the runoff profiles approaches the average, \bar{Q} , that is representative of the entire watershed (Figure 7, black line, right axis). For example, for a storm event with average rainfall of $\bar{R}=61$ mm (Figure 7), the average runoff for the watershed area, $\bar{Q}=30.6$ mm, is the area under the threshold-excess profile of runoff, which is $\bar{Q}_t F_t$ where $\bar{Q}_t=72.3$ mm and $F_t=0.32$, plus the area under the prethreshold profile of runoff, which is $\bar{Q}_p (1-F_t)$ where $\bar{Q}_p=11.3$ mm. In Figure 7, the runoff profile curves of equations (28) and (29) have also been represented as averages for each of 10 equal partitions of the threshold-excess and prethreshold runoff areas.

6. Discussion

6.1. How the Framework Complements and Compares With the Traditional SCS-CN Method

The SCS-CN method is the standard spatially lumped procedure for event-based rainfall-runoff prediction. While the SCS-CN method is a simple and transparent procedure for runoff prediction, the method has

with threshold saturation, F_t . In this case, the average rainfall is the average threshold-excess runoff, i.e., $\bar{Q}_t = \bar{R}$ (see equation (B7)). Traditionally, the SCS-CN method is derived from the assumption that the ratio \bar{Q}/\bar{R} is equal to the ratio $(\bar{R}-\bar{Q})/\bar{S}$ [e.g., Ponce and Hawkins, 1996]. The new derivation shows that this assumption results from point values of exponentially distributed rainfall, R , exceeding point values of exponentially distributed antecedent potential retention (i.e., $S=cw$). For an analysis of the sensitivity of average runoff to average rainfall, see Appendix A.

5.4. Examining the Spatial Variability of Runoff

To examine runoff variability, we use the quantile functions of the prethreshold and

threshold-excess runoff PDFs.

The quantile function equals the maximum value of runoff found within a

fraction of the watershed area, F .

For F from 0 to 1, the quantile functions show the variability of the runoff

depth over the watershed.

Here we consider two watershed areas: (1) the fraction of area between 0 and

F_t where threshold-excess runoff occurs and (2) the fraction of area between

F_t and 1 where prethreshold runoff occurs (Figure 7).

For the fraction of area with threshold-excess runoff, i.e., $0 \leq F \leq F_t$, the

quantile function,

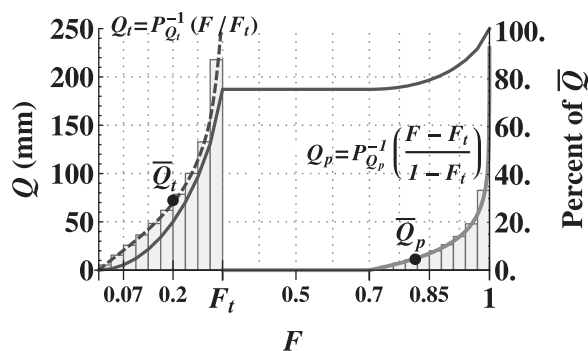


Figure 7. The average runoff for 10 equal partitions (gray bars) of the fraction of area with threshold-excess runoff F_t , and 10 equal partitions (gray bars) of fraction of area with prethreshold runoff, $\beta(1-F_t)$, where the fraction of area $(1-F_t)(1-\beta)$ produces zero prethreshold runoff. The continuous profile of threshold-excess runoff (black dashed line, equation (28)) and prethreshold runoff (gray line, equation (29)), as well as the percent of runoff produced in a fraction of the watershed area (black line). Results are for $\beta=0.45$, $\bar{c}=0.4$, $\bar{w}=240$ mm, and $R=61$ mm, where $F_t=0.32$ and $\bar{Q}=30.6$ mm.

several shortcomings and thus many recent calls have been made for rethinking the approach [Hawkins, 2014]. Nevertheless, it has been applied well beyond its original intended use and is found in water quality, sediment erosion, and environmental impact models [Garen and Moore, 2005; Beven, 2012]. These models are applied across a variety of watersheds even though the empirical origins of the SCS-CN method restrict its application to specific geographic regions and watershed types. Equally problematic is that the SCS-CN method provides a spatially uniform runoff quantity, which may produce erroneous results for spatially variable runoff-mediated processes such as erosion [Garen and Moore, 2005].

Our new theoretical framework enables the construction of spatially lumped event-

based models based on an assumed rainfall-runoff response at a point and a joint PDF that describes the spatial variability of the watershed system for a storm event. From this PDF, one can then derive the spatial variability of runoff as well as the average runoff value, i.e., the so-called “runoff curve.” The theoretical framework assumes that (1) rainfall is statistically independent from soil moisture, (2) the rainfall-runoff response at a point is described by a deterministic function of the watershed variables, and (3) the PDF of the antecedent soil moisture deficit, $p_{c|w}(c|w)$, may be linked to the average \bar{c} through the approximation $\hat{p}_{c|w}(c|w; \bar{c})$ of equation (12).

While the assumption of statistically independent rainfall may be reasonable for small watersheds, at the regional scale some studies have shown a correlation between soil moisture and rainfall [D’Odorico and Porporato, 2004]. In addition, in mountainous regions, rainfall may be correlated with elevation. In such instances, the rainfall-runoff response could be probabilistic. Such an assumption necessitates that the deterministic rainfall-runoff response described by the point mass of probability of equation (6) be replaced with a PDF description for a distribution representing a variable runoff quantity for given watershed variables. Though we assume a very simple functional dependence between the PDF $\hat{p}_{c|w}(c|w; \bar{c})$ and the average watershed value \bar{c} , in reality, the functional dependency may represent more complex behavior such as a hysteresis of the soil moisture deficit variability with fluctuating \bar{c} .

Following the ProStor framework, we created the new SCS-CN_x method by assuming the rainfall-runoff responses of equations (14) and (15) and the unique distributions of $p_R(R)$ and $\hat{p}_{cw}(c, w; \bar{c})$ of equations (22) and (23), respectively. The traditional SCS-CN method has a basis in the data from small experimental watersheds. Likewise, the PDFs used to derive the SCS-CN_x method are most applicable to smaller watersheds. The PDF $\hat{p}_{cw}(c, w; \bar{c})$ of equation (23) assumes homogeneous soil moisture over the watershed, while the rainfall PDF of equation (22) is most suitable for watersheds less than 40 km². However, these distributions also may hold for larger watersheds where vegetation homogenizes the spatial variability of soil moisture and where storm event rainfall typically is widespread and not patchy in distribution. According to the rainfall-runoff response of equations (14) and (15), the model now includes prethreshold runoff and threshold-excess runoff. When the prethreshold runoff is zero ($\beta = 0$), the new SCS-CN_x method reduces to the traditional SCS-CN method.

Existing studies have alluded to the prethreshold and threshold-excess runoff mechanisms [e.g., Bartlett et al., 2015; McMillan et al., 2014, Figures 6 and 7] and further studies are needed to quantify the threshold-excess and prethreshold runoff components of a storm event. Such studies may account for the threshold-excess runoff from both the hillslope and adjacent saturated riparian areas and thus allow for a quantification of the prethreshold runoff component. The prethreshold runoff occurs over the fraction of area β , and additional work also may determine if β changes seasonally or with different climate conditions. Such changes may link β to \bar{c} , and both β and the spatial variability of soil moisture may have a hysteretic

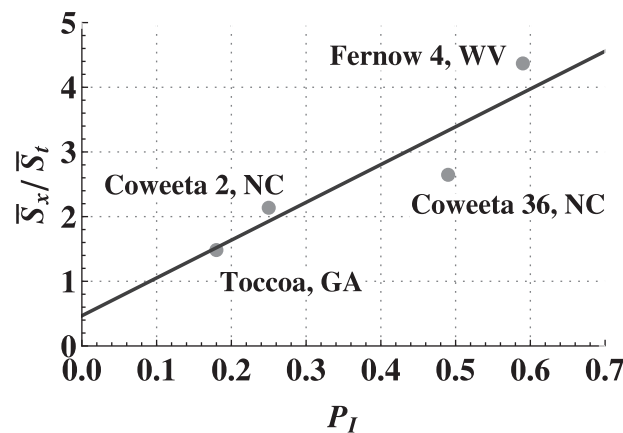


Figure 8. For the case study areas, the ratio of the antecedent potential values for the extended and traditional SCS-CN methods, i.e., \bar{S}_x and \bar{S}_r , respectively, versus the prethreshold runoff index, P_I . The linear regression (black line) shows the relationship $\bar{S}_x/\bar{S}_r = 5.8P_I + 0.46$.

new prethreshold runoff index parameter, $P_I = \beta(1 - \bar{c})$. The value of P_I may correlate to climate, stream order, or vegetation density. Based on such correlations, P_I potentially could be referenced from tables according to the site and climate conditions of an ungauged watershed. Because of the new parameter P_I , the optimal \bar{S} for the new SCS-CN_x method is different from the optimal value for the traditional SCS-CN method. Consequently, values of \bar{S} referenced from the existing CN tables are only valid for the traditional SCS-CN method, and for the new SCS-CN_x method, these values of \bar{S} should be modified to account for P_I . For example, the values of the traditional and extended methods could be related to P_I through a linear relationship with two parameters a and b , i.e.,

$$\bar{S}_x = \bar{S}_r(aP_I + b), \tag{30}$$

where based on P_I , the antecedent potential retention of the SCS-CN_x method, \bar{S}_x , is found from the traditional SCS-CN method value, \bar{S}_r , referenced from the existing CN tables. For the forested case study watersheds, $a = 5.8$ and $b = 0.46$ based on a satisfactory linear regression (see Figure 8).

The new SCS-CN_x method includes a spatial description of runoff that was missing from the traditional SCS-CN method. This description includes the source areas of runoff and the PDF characterizing the variability of runoff. While a source area of runoff was considered by Steenhuis *et al.* [1995], we now consider runoff to be a variable depth over two source areas for prethreshold runoff and threshold-excess runoff, respectively. Therefore, in the newly presented theoretical framework, the runoff producing area is equal to the fraction of the watershed with threshold-excess runoff, F_t , plus the fraction of the watershed with prethreshold runoff, $(1 - F_t)\beta$. Without the spatial description of runoff variability, spatially lumped event-based runoff is typically considered to be a uniform depth over the watershed area [Garen and Moore, 2005; Hawkins, 1982]. This new characterization of runoff variability should be particularly useful in improving models of erosion and water quality that rely on event-based runoff predictions (e.g., the SCS-CN method). For example, a point description of erosion may now be integrated over the runoff PDF of equation (25) to determine an average value of watershed erosion for a storm event.

6.2. Improved Model Representation of Rainfall-Runoff Data

The parameters of the new SCS-CN_x method and traditional SCS-CN methods are based on a nonlinear least squares fit to the case study data (see Figure 9 and Table 2). For the traditional SCS-CN method, the best fit results in zero initial abstraction (i.e., $\mu = 0$). Before fitting each model, the data were sorted on a rank-order basis, resulting in rainfall-runoff pairs that are frequency matched [Tedela *et al.*, 2011; Hawkins, 1993] (see Appendix D). Because the rainfall-runoff pairs are frequency matched, runoff typically is not paired with its causative rainfall event, but this data processing reveals the approximate form of the observed rainfall-runoff curve when the watershed antecedent soil moisture deficit, \bar{c} , is approximately equal to the temporal average, i.e., $\bar{c} \approx \langle \bar{c} \rangle$ (see Appendix D). Consequently, the rank-order data also represent the runoff

dependence on \bar{c} . In addition, we hypothesize that the prethreshold runoff may translate through the soil to the stream variable source area (VSA) [Hewlett and Hibbert, 1967], so it could represent an “old” water component of runoff that may be identified by an isotopic/solute mass balance hydrograph separation [e.g., McGlynn and McDonnell, 2003].

In this framework, the antecedent potential retention, \bar{S} , is represented by the product of the average antecedent soil moisture deficit and the storage capacity, i.e., $\bar{c}\bar{w}$. The average \bar{w} is considered a constant while \bar{c} varies between 0 and 1 over time due to ecohydrological controls. The new model runoff curve of equation (26) is governed by \bar{S} and the

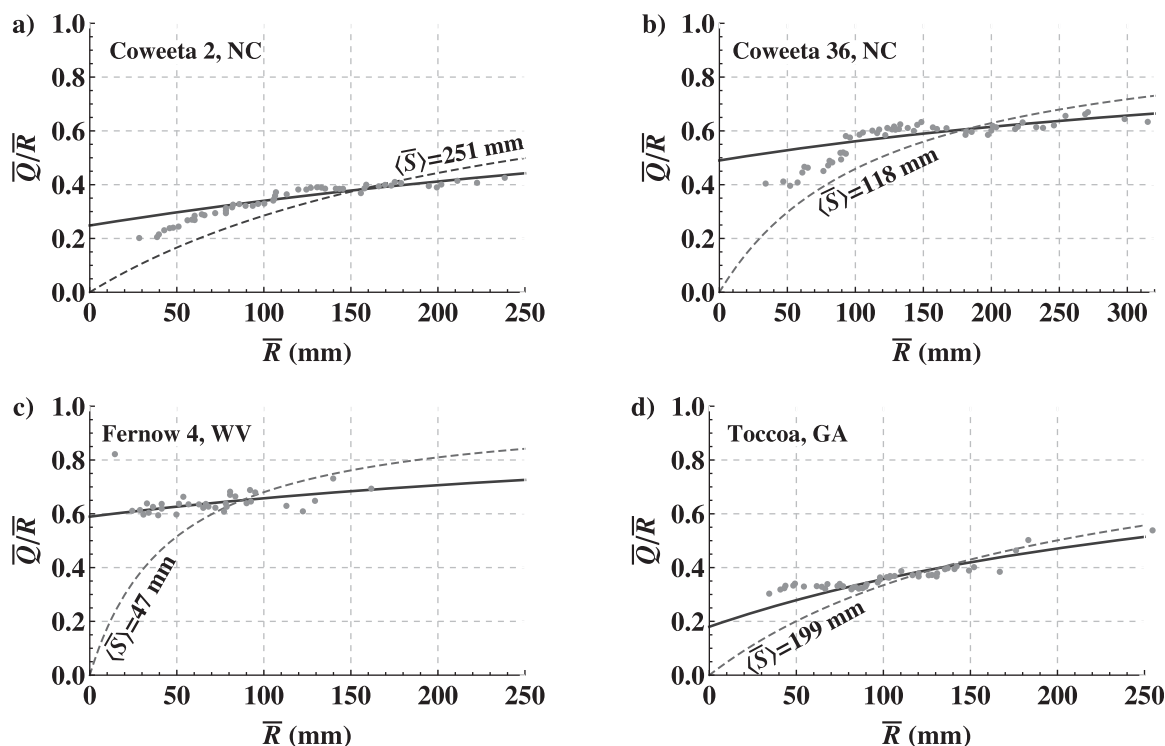


Figure 9. Comparison of runoff coefficients from rank-order data (gray dots), the new SCS-CN_x method (solid line) of equation (26), and the traditional SCS-CN method (dashed line) of equation (1) for the displayed $\langle \bar{S} \rangle$, which is based on a nonlinear least squares fit of equation (1) to the data. In all cases, the best fit occurs when the initial abstraction is zero for equation (1), i.e., $\bar{T} = 0$. See Table 2 for the SCS-CN_x method parameters of $\langle \bar{S} \rangle$ and $\langle P_t \rangle$. The rank-order data are reproduced from *Tedela et al.* [2011, 2008].

response for the temporal averages of the watershed antecedent potential retention, $\langle \bar{S} \rangle$, and prethreshold runoff index, $\langle P_t \rangle$ (see Table 2).

For the four forested watersheds (Figure 9), the new SCS-CN_x method better represents the rainfall-runoff data and is a significant improvement over the traditional SCS-CN method as indicated by the root-mean-square error (RMSE) (Table 2). This improvement is related to the new runoff description via thresholds, which assumes some areas produce a prethreshold runoff that varies with the parameter $P_t = \beta(1 - \bar{c})$. Because of this parameter, the new SCS-CN_x method captures runoff from small rainfall events that do not activate large areas of threshold-excess runoff. Thus, in comparison to the traditional SCS-CN method, the SCS-CN_x method may predict larger runoff coefficients for smaller rainfall values (Figure 9). The SCS-CN_x method may be a better alternative for site types that have been misrepresented by the traditional SCS-CN method (e.g., the forested watersheds of Figure 9). Since the new SCS-CN_x method defaults to the traditional SCS-CN method when $\beta = 0$, it also may represent agricultural watersheds where traditional the SCS-CN method typically shows a high level of agreement with recorded data.

6.3. Physical Interpretation of the Runoff Response

In section 4.1, we consider the watershed as two areas, each with a different rainfall-runoff response based on thresholds. Over the fraction of area β , a prethreshold runoff production occurs before infiltration exceeds the storage capacity threshold (see equation (14)). Conversely, over the complementary fraction of area $1 - \beta$, runoff is zero before infiltration exceeds the storage capacity threshold (see equation (15)). These two areas may be representative of two watershed areas defined by different hydrologic connections to the stream. A hydrologic connection to the stream indicates a continuity of subsurface flow from the landscape point to the nearest downslope stream. The fraction of area β may be representative of riparian and lower hillslope that have a persistent connection to the stream that allows for rainfall to initiate prethreshold runoff, which we assume is a lateral translation of water to the stream VSA [Hewlett and Hibbert, 1967]. The fraction of area $1 - \beta$ may be representative of upslope areas where prethreshold runoff is zero because the connection to the stream episodically occurs when infiltration fills and then spills over the storage capacity

Table 2. The SCS-CN_x Method: Parameters and Root-Mean-Square Error (RMSE) Comparison

| Watershed | Area (ha) | $\langle \bar{S} \rangle = \langle \bar{c} \rangle \bar{w}^a$ (mm) | $\langle P_t \rangle = \beta \langle \bar{x} \rangle^a$ | SCS-CN _x RMSE ^b | SCS-CN RMSE ^b |
|---------------------|-----------|--|---|---------------------------------------|--------------------------|
| Coweeta 2, NC, USA | 12.3 | 540 | 0.25 | 0.029 | 0.060 |
| Coweeta 36, NC, USA | 46.6 | 314 | 0.49 | 0.049 | 0.081 |
| Fernow 4, WV, USA | 38.7 | 206 | 0.59 | 0.036 | 0.15 |
| Toccoa, GA, USA | 45842 | 298 | 0.18 | 0.029 | 0.067 |

^aParameter based on a nonlinear least squares fit of equation (26) to the rank-order rainfall-runoff data (see Appendix D).

^bRoot-mean-square error (RMSE) based on the runoff coefficients.

threshold [e.g., *Tromp-van Meerveld and McDonnell, 2006a*]. Though the runoff responses of the two areas differ in prethreshold runoff production, points in both areas have a storage capacity threshold.

The storage capacity threshold of equations (14) and (15) acts as a proxy for many different runoff mechanisms, e.g., overland flow by saturation or infiltration excess and subsurface stormflow, and thus implicit in the threshold descriptions of equations (14) and (15) is the notion that runoff processes are phenomenologically the same as outlined in *McDonnell [2013]* and as recently implemented numerically by *Ameli et al. [2016]*. During a rainfall event, overland flow emerges over saturated areas on poorly permeable soils [*Antoine et al., 2009; Fiedler and Ramirez, 2000*] or areas that become saturated from a rising permanent or perched water table [*Frei and Fleckenstein, 2014; Frei et al., 2010; Loague et al., 2010; Mirus and Loague, 2013*]. Subsurface flow is typically summarized as emerging from areas of transient saturation that develop at soil-bedrock interface [*Spence and Woo, 2003; Tromp-van Meerveld and McDonnell, 2006b*]. For all of these processes, the soil delays the development of an area of saturation and watershed points saturate and detain water until a storage capacity threshold. After this storage capacity threshold is exceeded, the point may be assumed to be part of a network of connected saturated areas that extend to the stream. This saturated area may be interpreted as the region where rainfall initiates a cascade of threshold-excess runoff that fills and spills as overland flow (typically near the stream) or as subsurface flow along the bedrock-soil interface in upslope areas [*McDonnell, 2003; McGlynn and McDonnell, 2003; Tromp-van Meerveld and McDonnell, 2006b*].

7. Concluding Remarks

We have presented a general theoretical framework (ProStor) for both creating spatially lumped rainfall-runoff response models of the same genus as the SCS-CN method and extending these models with a spatial description of runoff variability. We used a new runoff concept (based on thresholds) within the framework to create an extended SCS-CN method (SCS-CN_x) that moves beyond the traditional SCS-CN method limitations. Unlike the traditional SCS-CN method, the extended SCS-CN_x method consists of equations for the fractions of watershed area producing either prethreshold or threshold-excess runoff, the PDF describing the spatial variability of runoff, and the corresponding average runoff value (i.e., the runoff curve). This new spatial description of runoff may allow for a more realistic extension of the SCS-CN_x method to runoff related processes such as erosion and nonpoint source pollution transport. Furthermore, the spatial distribution of runoff may be mapped to the watershed based on a similarity index such as the topographic index [e.g., *Lyon et al., 2004*].

The extended SCS-CN_x method defaults to the traditional SCS-CN method when the prethreshold runoff behavior is negligible. In comparison to the traditional method, the extended method performs significantly better (with a lower RMSE) for four forested watersheds. The improvement is related to the new runoff description via thresholds, which assumes some areas produce a prethreshold runoff that varies with the new parameter called the prethreshold runoff index. This parameter allows the SCS-CN_x method to capture runoff from small rainfall events that do not activate large areas of threshold-excess runoff. Thus, this new model may better represent geographic regions and site types that previously have been beyond the scope of the traditional SCS-CN method. The prethreshold runoff index is the product of the average soil moisture over the watershed and the fraction of area β with a persistent hydrologic connection to the stream. Widespread implementation of the SCS-CN_x method will require further inquiry into how β varies with topography, soil type, vegetation, and other factors. In addition, both the extended and traditional models are now linked to the spatial distribution of soil moisture. This link to soil moisture paves the way toward modeling

the effect of ecohydrological processes on event-based rainfall-runoff predictions. Incorporating ecohydrological processes into event-based models may result in more accurate spatial descriptions of runoff and the average runoff curve value.

The ProStor framework may also be applied with different rainfall-runoff responses at a point and different spatial PDFs for the watershed variables. Widely used semidistributed models such as TOPMODEL, Variable Infiltration Capacity (VIC), and the Probability Distributed Model (PDM) use different distributions of variables to describe the watershed area. In lieu of the storage capacity distribution used in this work, we could use the Pareto (or Xinanjiang) distribution of VIC and PDM [Moore, 2007; Liang et al., 1994] or the gamma distribution of TOPMODEL [Sivapalan et al., 1987]. Thus, the ProStor framework could provide a means for unifying different hydrologic models as alternative versions of spatially lumped event-based models analogous to the traditional SCS-CN method and the new SCS-CN_x method.

Appendix A: Sensitivity of Average Runoff to Average Rainfall

For the runoff curve of equation (26) where $\bar{Q} = F_t \bar{Q}_t + (1 - F_t) \bar{Q}_p$, the change in the average runoff with respect to the average rainfall is

$$\frac{d\bar{Q}}{dR} = F_t \frac{d\bar{Q}_t}{dR} + \bar{Q}_t \frac{dF_t}{dR} + (1 - F_t) \frac{d\bar{Q}_p}{dR} - \bar{Q}_p \frac{dF_t}{dR}. \quad (A1)$$

As described by the first and third terms of the RHS of equation (A1), the average runoff increases because both threshold-excess runoff, \bar{Q}_t , and prethreshold runoff, \bar{Q}_p , increase with respect to rainfall. According to the RHS of equation (A1), the average runoff also changes because the fraction of threshold-excess area increases with rainfall (second term) while the fraction of prethreshold area decreases with rainfall (fourth term).

For the SCS-CN method of equation (27) where $\bar{Q} = F_t \bar{R}$, equation (A1) becomes

$$\frac{d\bar{Q}}{dR} = F_t + \bar{R} \frac{dF_t}{dR}. \quad (A2)$$

The two terms of the RHS of equation (A2), respectively represent the fraction of area with threshold-excess runoff, F_t , and the increase in this fraction because of rainfall, i.e., $\bar{R} dF_t/dR$. Thus, the average runoff, \bar{Q} , increases from rainfall over the area, F_t , and rainfall over the area that develops threshold-excess runoff because of rainfall, $\bar{R} dF_t/dR$. Because the fraction F_t changes with rainfall according to $\bar{R} dF_t/dR$, threshold-excess runoff, \bar{Q} , is the average of a variable runoff depth over the fraction of area F_t .

The work of Steenhuis et al. [1995] defined the fraction of contributing area as $d\bar{Q}/dR = F_t$. Thus, the contributing area, F_t , was considered to be a static and not variable with the average rainfall during the storm according to the term $\bar{R} dF_t/dR$. Consequently, the Steenhuis et al. [1995] model of a static contributing area also implies that the runoff depth is uniform. For the same runoff quantity, a uniform runoff depth [e.g., Steenhuis et al., 1995] necessitates that the contributing area be larger than when the runoff depth is variable (Figure 7). The runoff depth likely will be variable because of randomness in rainfall and watershed heterogeneities. Therefore, Steenhuis et al. [1995] likely overpredicts the extent of contributing area, which is smaller for the variable runoff depth description of our model framework (equation (24) and Figure 4a).

Appendix B: Prethreshold and Threshold-Excess Runoff PDFs and Averages

For the rainfall PDF of equation (22) and the antecedent soil moisture deficit and storage capacity PDF of equation (23), the specific form of the prethreshold runoff PDF of equation (19) is

$$p_{Q_p}(Q) = (1 - \beta) \delta(Q) + \frac{1}{1 - F_t} \left(\frac{\beta}{\bar{x}} p_R \left(\frac{Q}{\bar{x}} \right) \int_0^{w_{\max}} \int_{\frac{Q}{\bar{x}} \frac{(1 - \beta x)}{x}}^1 \delta(c - \bar{c}) \frac{1}{W} e^{-w/\bar{w}} dc dw \right), \quad (B1)$$

and integrating over the antecedent soil moisture deficit retrieves the expression

$$p_{Q_p}(Q) = (1 - \beta)\delta(Q) + \frac{1}{1 - F_t} \left(\frac{\beta}{\bar{x}} p_R \left(\frac{Q}{\bar{x}} \right) \int_0^{W_{\max}} \Theta \left(\bar{c} - \frac{Q(1 - \beta\bar{x})}{w} \right) \frac{1}{w} e^{-w/\bar{w}} dw \right). \quad (B2)$$

The argument of the step function, $\Theta(\cdot)$, sets the lower bound for integration over the storage capacity, w , i.e.,

$$p_{Q_p}(Q) = (1 - \beta)\delta(Q) + \frac{1}{1 - F_t} \left(\frac{\beta}{\bar{x}} p_R \left(\frac{Q}{\bar{x}} \right) \int_{\frac{Q(1 - \beta\bar{x})}{\bar{c}}}^{W_{\max}} \frac{1}{w} e^{-w/\bar{w}} dw \right), \quad (B3)$$

and integrating over w results in the prethreshold runoff PDF

$$p_{Q_p}(Q) = (1 - \beta)\delta(Q) + \frac{\beta}{1 - F_t} \left(\frac{e^{-Q \frac{1}{(1 - F_t)(1 - \bar{c})\bar{R}}}}{\bar{R}(1 - \bar{c})} \right), \quad (B4)$$

where $0 \leq Q < \infty$ and $1/(1 - F_t)$ is the normalization constant for the PDF, the delta function of the first term indicates an atom of finite probability for zero runoff, $p_{Q_p}(Q=0)$, for the fraction of area, $1 - \beta$, and the second term represents the distribution of prethreshold runoff over the fraction of area, β . For the limiting case of $\beta = 0$, $p_{Q_p}(Q) = \delta(Q)$, which indicates that there is a discrete probability of zero runoff over the fraction of area, $1 - F_t$.

For the PDF of equation (22) and antecedent soil moisture deficit and storage capacity PDF of equation (23), the specific form of the threshold-excess runoff PDF of equation (20) is first integrated over c , and by the sifting property of the delta function, the average \bar{c} is substituted for c . Subsequently integrating over w then results in the threshold-excess runoff PDF

$$p_{Q_t}(Q) = (1 - \beta) \frac{1}{\bar{R}} e^{-\frac{Q}{\bar{R}}} + \frac{\beta}{F_t} e^{-\frac{Q}{\bar{R}}} (1 - (1 - \bar{c})\beta) \frac{1 - e^{-\frac{Q^2 \bar{w} + \bar{R}(1 - (1 - \bar{c})\beta)}{c w (1 - \bar{c})\bar{R}}}}{c^2 \bar{w} + \bar{R}(1 - (1 - \bar{c})\beta)}, \quad (B5)$$

where $0 \leq Q < \infty$ and $1/F_t$ is the normalization constant for the PDF. For the limiting case of $\beta = 0$, the threshold-excess runoff PDF becomes $p_{Q_t}(Q) = (1/F_t) e^{-Q/\bar{R}} / (\bar{c}\bar{w} + \bar{R})$.

Over the fraction of area $1 - F_t$, the average (unit area) prethreshold runoff from the PDF of equation (B4) is

$$\bar{Q}_p = (1 - F_t) \bar{R} (1 - \bar{c}) \beta, \quad (B6)$$

while over the fraction of area F_t , the average (unit area) threshold-excess runoff from the PDF of equation (B5) is

$$\bar{Q}_t = (1 - F_t) (1 + (1 - \bar{c})\beta) \bar{R} + F_t \bar{R}, \quad (B7)$$

and multiplying the averages \bar{Q}_t and \bar{Q}_p by the fractions F_t and $1 - F_t$, respectively, normalizes the values to a unit watershed area and recovers $\bar{Q} = F_t \bar{Q}_t + (1 - F_t) \bar{Q}_p$.

Appendix C: Cumulative Distribution and Quantile Functions

The cumulative probability distribution (CDF) for the entire watershed area is the weighted sum of the CDFs for prethreshold runoff, $P_{Q_p}(Q_p)$, and threshold-excess runoff, $P_{Q_t}(Q_t)$, i.e.,

$$P_Q(Q) = (1 - F_t) P_{Q_p}(Q) + F_t P_{Q_t}(Q). \quad (C1)$$

For the prethreshold runoff PDF of equation (B4), the CDF is

$$P_{Q_p}(Q) = 1 - \beta + \beta \left(1 - e^{-Q \frac{1}{(1 - F_t)(1 - \bar{c})\bar{R}}} \right). \quad (C2)$$

Based on equation (B5) PDF, the threshold-excess runoff CDF is

$$P_{Q_t}(Q) = 1 - e^{-\frac{Q}{\bar{R}}} + \beta e^{-\frac{Q}{\bar{R}}} \bar{c} \bar{w} (1 - \bar{c}) \frac{e^{-\frac{Q^2 \bar{w} + \bar{R}(1 - (1 - \bar{c})\beta)}{c w (1 - \bar{c})\bar{R}}} - 1}{c^2 \bar{w} + \bar{R}(1 - (1 - \bar{c})\beta)}. \quad (C3)$$

The quantile function, which is the inverse CDF, provides the maximum runoff value found within a fraction of the watershed area. For prethreshold runoff, the quantile function of equation (C2) CDF is

$$P_{Q_p}^{-1}(F) = \begin{cases} 0 & \text{for } 0 \leq F < 1 - \beta \\ (1 - F_t)(1 - \bar{c}) \bar{R} \ln \left(\frac{\beta}{1 - F} \right) & 1 - \beta \leq F < 1, \end{cases} \quad (C4)$$

where F represents the fraction the area with prethreshold runoff, and prethreshold runoff is zero for the fraction of area $1 - \beta$. For threshold-excess runoff, the CDF of equation (C3) may not be inverted, except for the case when $\beta = 0$, for which the quantile function is

$$P_{Q_t, \beta=0}^{-1}(F) = \bar{R} \ln \left(\frac{1}{1 - F} \right), \quad (C5)$$

where F represents a fraction of the area with threshold-excess runoff.

Appendix D: Rank-Order Data Approximation of the Runoff Curve

Rank-order rainfall and runoff pairs are found from the original data by listing the rainfall and runoff values in descending order and pairing the ordered values. The rank-order data then reveal a transformation between the rainfall and runoff depth distributions $p_{\bar{R}}(\bar{R})$ and $p_{\bar{Q}}(\bar{Q})$. We will now show that this transformation described by the rank-order data is approximately the runoff curve, e.g., equation (26), when \bar{c} is set equal to the temporal average, i.e., $\bar{c} = \langle \bar{c} \rangle$.

For a series of storm events, the runoff distribution $p_{\bar{Q}}(\bar{Q})$, may be found by transforming the rainfall distribution, $p_{\bar{R}}(\bar{R})$, i.e., [Bartlett et al., 2015]

$$p_{\bar{Q}}(\bar{Q}) = \int_0^{\infty} p_{\bar{Q}|\bar{R}}(\bar{Q}|\bar{R}) p_{\bar{R}}(\bar{R}) d\bar{R}, \quad (D1)$$

where the conditional distribution $p_{\bar{Q}|\bar{R}}(\bar{Q}|\bar{R})$ represents a probabilistic transformation of rainfall, \bar{R} , to runoff, \bar{Q} . The transformation $p_{\bar{Q}|\bar{R}}(\bar{Q}|\bar{R})$ is based on the runoff curve response, $\bar{Q}(\bar{R}, \bar{c})$, and the distribution of $p_{\bar{c}}(\bar{c})$, i.e.,

$$p_{\bar{Q}|\bar{R}}(\bar{Q}|\bar{R}) = \int_0^1 \delta(\bar{Q}(\bar{R}, \bar{c}) - \bar{Q}) p_{\bar{c}}(\bar{c}) d\bar{c} = E_{\bar{c}} [p_{\bar{Q}|\bar{R}\bar{c}}(\bar{Q}|\bar{R}, \bar{c})], \quad (D2)$$

where the Dirac delta function, $\delta(\cdot)$, represents a point mass of probability, i.e., runoff always assumes the value of $\bar{Q}(\bar{R}, \bar{c})$, and this discrete probability is weighted by the multiple wetness states described by the distribution $p_{\bar{c}}(\bar{c})$. The point mass $\delta(\bar{Q}(\bar{R}, \bar{c}) - \bar{Q})$ represents the conditional PDF $p_{\bar{Q}|\bar{R}\bar{c}}(\bar{Q}|\bar{R}, \bar{c})$, and equation (D2) may be equivalently viewed as the expected value, $E_{\bar{c}}[\cdot]$, of this conditional distribution, $p_{\bar{Q}|\bar{R}\bar{c}}(\bar{Q}|\bar{R}, \bar{c})$.

We may approximate the transformation of equation (D2) by noting that for the range over which \bar{c} varies, the runoff curve $\bar{Q}(\bar{R}, \bar{c})$ is approximately linear with \bar{c} , and therefore

$$E_{\bar{c}} [p_{\bar{Q}|\bar{R}\bar{c}}(\bar{Q}|\bar{R}, \bar{c})] \approx p_{\bar{Q}|\bar{R}\bar{c}}(\bar{Q}|\bar{R}, E[\bar{c}]), \quad (D3)$$

where the expected value $E[\bar{c}]$ is the temporal average $\langle \bar{c} \rangle$. Consequently, the probabilistic transformation of rainfall to runoff becomes

$$p_{\bar{Q}|\bar{R}}(\bar{Q}|\bar{R}) \approx \delta(\bar{Q}(\bar{R}, \langle \bar{c} \rangle) - \bar{Q}), \quad (D4)$$

and when this expression is inserted back into equation (D1), equation (D1) then represents an alternative form of a distribution transformation by the change of variables technique [e.g., Bendat and Piersol, 2011; Gillespie, 1983; Au and Tam, 1999] where the delta function is evaluated using the property of Appendix E. Following equations (D1) and (D4), the runoff distribution is approximately the rainfall distribution transformed by the runoff curve for the case of $\bar{c} = \langle \bar{c} \rangle$. As a result, the rank-order data thus approximately show the runoff curve $\bar{Q}(\bar{R}, \langle \bar{c} \rangle)$.

Appendix E: Dirac Delta Function Property

When integrating equation (8), the Dirac delta function of equation (7) often cannot be evaluated explicitly using the sifting property but may be evaluated (in this case for the variable of integration R) with the property

$$\delta[g(R)] = \sum_n \frac{1}{|g'(R_n)|} \delta(R - R_n), \quad (E1)$$

where $g(R)$ is the function nested within the delta function, i.e., $g(R) = Q(R, c, w) - Q$; the summation is for all the roots R_n where $g(R_n) = 0$; and $g'(\cdot)$ is the derivative of the function with respect to R [e.g., *Au and Tam, 1999*].

Acknowledgments

This work was supported through the USDA Agricultural Research Service cooperative agreement 58-6408-3-027; and National Science Foundation (NSF) grants CBET-1033467, EAR-1331846, FESD-1338694, EAR-1316258, and the Duke WISENet grant DGE-1068871. The data used for Figure 9 are reproduced from *Tedela et al.* [2011, 2008]. Processed data and code are available by e-mail from the corresponding author. We thank the reviewers for their useful and constructive comments that helped improve the paper.

References

- Ajami, N. K., H. Gupta, T. Wagener, and S. Sorooshian (2004), Calibration of a semi-distributed hydrologic model for streamflow estimation along a river system, *J. Hydrol.*, *298*(1), 112–135.
- Ali, G., C. J. Oswald, C. Spence, E. L. Cammeraat, K. J. McGuire, T. Meixner, and S. M. Reaney (2013), Towards a unified threshold-based hydrological theory: Necessary components and recurring challenges, *Hydrol. Processes*, *27*(2), 313–318.
- Ameli, A. A., J. R. Craig, and J. J. McDonnell (2016), Are all runoff processes the same? Numerical experiments comparing a Darcy-Richards solver to an overland flow-based approach for subsurface storm runoff simulation, *Water Resour. Res.*, *51*, 10,008–10,028, doi:10.1002/2015WR017199.
- Antoine, M., M. Javaux, and C. Bièdiers (2009), What indicators can capture runoff-relevant connectivity properties of the micro-topography at the plot scale?, *Adv. Water Resour.*, *32*(8), 1297–1310.
- Arnell, N. (2014), *Hydrology and Global Environmental Change, Understanding Global Environmental Change*, Taylor and Francis, N. Y.
- Au, C., and J. Tam (1999), Transforming variables using the Dirac generalized function, *Am. Stat.*, *53*(3), 270–272.
- Bartlett, M. S., E. Daly, J. J. McDonnell, A. J. Parolari, and A. Porporato (2015), Stochastic rainfall-runoff model with explicit soil moisture dynamics, in *Proc. R. Soc. A*, *471*, doi:10.1098/rspa.2015.0389.
- Bendat, J. S., and A. G. Piersol (2011), *Random Data: Analysis and Measurement Procedures*, vol. 729, John Wiley, Hoboken, N. J.
- Beven, K. (2012), *Rainfall-Runoff Modelling: The Primer*, John Wiley, Hoboken, N. J.
- Beven, K., and M. Kirkby (1979), A physically based, variable contributing area model of basin hydrology/un modèle à base physique de zone d'appel variable de l'hydrologie du bassin versant, *Hydrol. Sci. J.*, *24*(1), 43–69.
- Cantón, Y., A. Solé-Benet, J. De Vente, C. Boix-Fayos, A. Calvo-Cases, C. Asensio, and J. Puigdefábregas (2011), A review of runoff generation and soil erosion across scales in semiarid south-eastern Spain, *J. Arid Environ.*, *75*(12), 1254–1261.
- Carpenter, S. R., N. F. Caraco, D. L. Correll, R. W. Howarth, A. N. Sharpley, and V. H. Smith (1998), Nonpoint pollution of surface waters with phosphorus and nitrogen, *Ecol. Appl.*, *8*(3), 559–568.
- Clark, M. P., A. G. Slater, D. E. Rupp, R. A. Woods, J. A. Vrugt, H. V. Gupta, T. Wagener, and L. E. Hay (2008), Framework for understanding structural errors (fuse): A modular framework to diagnose differences between hydrological models, *Water Resour. Res.*, *44*, W00B02, doi:10.1029/2007WR006735.
- D'Odorico, P., and A. Porporato (2004), Preferential states in soil moisture and climate dynamics, *Proc. Natl. Acad. Sci. U. S. A.*, *101*(24), 8848–8851.
- Famiglietti, J. S., D. Ryu, A. A. Berg, M. Rodell, and T. J. Jackson (2008), Field observations of soil moisture variability across scales, *Water Resour. Res.*, *44*, W01423, doi:10.1029/2006WR005804.
- Fatichi, S., G. G. Katul, V. Y. Ivanov, C. Pappas, A. Paschalis, A. Consolo, J. Kim, and P. Burlando (2015), Abiotic and biotic controls of soil moisture spatiotemporal variability and the occurrence of hysteresis, *Water Resour. Res.*, *51*, 3505–3524, doi:10.1002/2014WR016102.
- Fatichi, S., et al. (2016), An overview of current applications, challenges, and future trends in distributed process-based models in hydrology, *J. Hydrol.*, *537*, 45–60.
- Fenicia, F., D. Kavetski, and H. H. Savenije (2011), Elements of a flexible approach for conceptual hydrological modeling: 1. Motivation and theoretical development, *Water Resour. Res.*, *47*, W11510, doi:10.1029/2010WR010174.
- Fiedler, F. R., and J. A. Ramirez (2000), A numerical method for simulating discontinuous shallow flow over an infiltrating surface, *Int. J. Numer. Methods Fluids*, *32*(2), 219–239.
- Frei, S., and J. H. Fleckenstein (2014), Representing effects of micro-topography on runoff generation and sub-surface flow patterns by using superficial rill/depression storage height variations, *Environ. Modell. Software*, *52*, 5–18.
- Frei, S., G. Lischeid, and J. Fleckenstein (2010), Effects of micro-topography on surface–subsurface exchange and runoff generation in a virtual riparian wetland—A modeling study, *Adv. Water Resour.*, *33*(11), 1388–1401.
- Garen, D. C., and D. S. Moore (2005), Curve number hydrology in water quality modeling: Uses, abuses, and future directions¹, *J. Am. Water Resour. Assoc.*, *41*(2), 377–388.
- Gillespie, D. T. (1983), A theorem for physicists in the theory of random variables, *Am. J. Phys.*, *51*(6), 520–533.
- Hawkins, R. H. (1982), Distribution of loss rates implicit in the SCS runoff equation, in *Hydrology and Water Resources in Arizona and the Southwest*, Arizona-Nevada Acad. of Sci., Fort Collins, Colo.
- Hawkins, R. H. (1993), Asymptotic determination of runoff curve numbers from data, *J. Irrig. Drain. Eng.*, *119*(2), 334–345.
- Hawkins, R. H. (2014), Curve number method: Time to think anew?, *J. Hydrol. Eng.*, *19*, 1059.
- Hewlett, J. D., and A. R. Hibbert (1967), Factors affecting the response of small watersheds to precipitation in humid areas, in *Forest Hydrology*, pp. 275–290, Pergamon Press, U. K.
- Hopp, L., and J. McDonnell (2009), Connectivity at the hillslope scale: Identifying interactions between storm size, bedrock permeability, slope angle and soil depth, *J. Hydrol.*, *376*(3), 378–391.
- Ivanov, V. Y., E. R. Vivoni, R. L. Bras, and D. Entekhabi (2004), Catchment hydrologic response with a fully distributed triangulated irregular network model, *Water Resour. Res.*, *40*, W11102, doi:10.1029/2004WR003218.
- Ivanov, V. Y., S. Fatichi, G. D. Jenerette, J. F. Espeleta, P. A. Troch, and T. E. Huxman (2010), Hysteresis of soil moisture spatial heterogeneity and the “homogenizing” effect of vegetation, *Water Resour. Res.*, *46*, W09521, doi:10.1029/2009WR008611.

- Jaynes, E., and G. Bretthorst (2003), *Probability Theory: The Logic of Science*, Cambridge Univ. Press, Cambridge, U. K.
- Kim, H. J., R. C. Sidle, and R. Moore (2005), Shallow lateral flow from a forested hillslope: Influence of antecedent wetness, *Catena*, 60(3), 293–306.
- Liang, X., D. P. Lettenmaier, E. F. Wood, and S. J. Burges (1994), A simple hydrologically based model of land surface water and energy fluxes for general circulation models, *J. Geophys. Res.*, 99(D7), 14,415–14,428.
- Liang, X., D. P. Lettenmaier, E. F. Wood, and S. Burges (1996), One-dimensional statistical dynamic representation of subgrid spatial variability of precipitation in the two-layer Variable Infiltration Capacity model, *J. Geophys. Res.*, 101(21), 403–21.
- Lin, H. (2012), *Hydropedology: Synergistic Integration of Soil Science and Hydrology*, Academic, Waltham, Mass.
- Lindström, G., B. Johansson, M. Persson, M. Gardelin, and S. Bergström (1997), Development and test of the distributed hbv-96 hydrological model, *J. Hydrol.*, 201(1), 272–288.
- Loague, K., C. S. Heppner, B. A. Ebel, and J. E. VanderKwaak (2010), The quixotic search for a comprehensive understanding of hydrologic response at the surface: Horton, Dunne, Dunton, and the role of concept-development simulation, *Hydrol. Processes*, 24(17), 2499–2505.
- Lyon, S. W., M. T. Walter, P. Gérard-Marchant, and T. S. Steenhuis (2004), Using a topographic index to distribute variable source area runoff predicted with the SCS curve-number equation, *Hydrol. Processes*, 18(15), 2757–2771.
- McDonnell, J., et al. (2007), Moving beyond heterogeneity and process complexity: A new vision for watershed hydrology, *Water Resour. Res.*, 43, W07301, doi:10.1029/2006WR005467.
- McDonnell, J. J. (2003), Where does water go when it rains? Moving beyond the variable source area concept of rainfall-runoff response, *Hydrol. Processes*, 17(9), 1869–1875.
- McDonnell, J. J. (2013), Are all runoff processes the same?, *Hydrol. Processes*, 27(26), 4103–4111.
- McGlynn, B. L., and J. J. McDonnell (2003), Quantifying the relative contributions of riparian and hillslope zones to catchment runoff, *Water Resour. Res.*, 39(11), 1310, doi:10.1029/2003WR002091.
- McMillan, H., M. Gueguen, E. Grimon, R. Woods, M. Clark, and D. E. Rupp (2014), Spatial variability of hydrological processes and model structure diagnostics in a 50 km² catchment, *Hydrol. Processes*, 28(18), 4896–4913.
- Mirus, B. B., and K. Loague (2013), How runoff begins (and ends): Characterizing hydrologic response at the catchment scale, *Water Resour. Res.*, 49, 2987–3006, doi:10.1002/wrcr.20218.
- Mirus, B. B., B. A. Ebel, C. S. Heppner, and K. Loague (2011), Assessing the detail needed to capture rainfall-runoff dynamics with physics-based hydrologic response simulation, *Water Resour. Res.*, 47, W00H10, doi:10.1029/2010WR009906.
- Mishra, S. K., and V. P. Singh (1999), Another look at SCS-CN method, *J. Hydrol. Eng.*, 4(3), 257–264.
- Moore, R. (2007), The PDM rainfall-runoff model, *Hydrol. Earth Syst. Sci.*, 11(1), 483–499.
- Naiman, R. J., T. J. Beechie, L. E. Benda, D. R. Berg, P. A. Bisson, L. H. MacDonald, M. D. O'Connor, P. L. Olson, and E. A. Steel (1992), Fundamental elements of ecologically healthy watersheds in the pacific northwest coastal ecoregion, in *Watershed Management*, pp. 127–188, Springer, N. Y.
- Paniconi, C., and M. Putti (2015), Physically based modeling in catchment hydrology at 50: Survey and outlook, *Water Resour. Res.*, 51, 7090–7129, doi:10.1002/2015WR017780.
- Pathak, C. S., R. S. Teegavarapu, C. Olson, A. Singh, A. W. Lal, C. Polatel, V. Zahraeifard, and S. U. Senarath (2015), Uncertainty analyses in hydrologic/hydraulic modeling: Challenges and proposed resolutions, *J. Hydrol. Eng.*, 20(10), 02515,003.
- Ponce, V. M., and R. H. Hawkins (1996), Runoff curve number: Has it reached maturity?, *J. Hydrol. Eng.*, 1(1), 11–19.
- Rallison, R. E., and N. Miller (1982), Past, present, and future SCS runoff procedure, in *Rainfall-Runoff Relationship/Proceedings, International Symposium on Rainfall-Runoff Modeling*, edited by V. P. Singh, pp. 353–364, Water Resour. Publ., Littleton, Colo.
- Rigby, J., and A. Porporato (2006), Simplified stochastic soil-moisture models: A look at infiltration, *Hydrol. Earth Syst. Sci.*, 10, 861–871.
- Rodríguez-Iturbe, I., and A. Porporato (2004), *Ecohydrology of Water-Controlled Ecosystems: Soil Moisture and Plant Dynamics*, Cambridge Univ. Press, Cambridge, U. K.
- Rodríguez-Iturbe, I., G. K. Vogel, R. Rigon, D. Entekhabi, F. Castelli, and A. Rinaldo (1995), On the spatial organization of soil moisture fields, *Geophys. Res. Lett.*, 22(20), 2757–2760.
- Ryu, D., and J. S. Famiglietti (2005), Characterization of footprint-scale surface soil moisture variability using Gaussian and beta distribution functions during the southern great plains 1997 (sgp97) hydrology experiment, *Water Resour. Res.*, 41, W12433, doi:10.1029/2004WR003835.
- Schaake, J. C., V. I. Koren, Q.-Y. Duan, K. Mitchell, and F. Chen (1996), Simple water balance model for estimating runoff at different spatial and temporal scales, *J. Geophys. Res.*, 101(D3), 7461–7475.
- Semenova, O., and K. Beven (2015), Barriers to progress in distributed hydrological modelling, *Hydrol. Processes*, 29(8), 2074–2078.
- Shuttleworth, W. J. (1988), Macrohydrology—The new challenge for process hydrology, *J. Hydrol.*, 100(1), 31–56.
- Sidle, R. C., Y. Tsuboyama, S. Noguchi, I. Hosoda, M. Fujieda, and T. Shimizu (2000), Stormflow generation in steep forested headwaters: A linked hydrogeomorphic paradigm, *Hydrol. Processes*, 14(3), 369–385.
- Sivakumar, B., and V. Singh (2012), Hydrologic system complexity and nonlinear dynamic concepts for a catchment classification framework, *Hydrol. Earth Syst. Sci.*, 16(11), 4119–4131.
- Sivakumar, B., V. P. Singh, R. Berndtsson, and S. K. Khan (2013), Catchment classification framework in hydrology: Challenges and directions, *J. Hydrol. Eng.*, 20, A4014002.
- Sivapalan, M., K. Beven, and E. F. Wood (1987), On hydrologic similarity: 2. A scaled model of storm runoff production, *Water Resour. Res.*, 23(12), 2266–2278.
- Sivapalan, M., E. F. Wood, and K. J. Beven (1990), On hydrologic similarity: 3. A dimensionless flood frequency model using a generalized geomorphologic unit hydrograph and partial area runoff generation, *Water Resour. Res.*, 26(1), 43–58.
- Sivapalan, M., R. A. Woods, and J. D. Kalma (1997), Variable bucket representation of TOPMODEL and investigation of the effects of rainfall heterogeneity, *Hydrol. Processes*, 11(9), 1307–1330.
- Spence, C., and M.-k. Woo (2003), Hydrology of subarctic Canadian shield: Soil-filled valleys, *J. Hydrol.*, 279(1), 151–166.
- Steenhuis, T. S., M. Winchell, J. Rossing, J. A. Zollweg, and M. F. Walter (1995), SCS runoff equation revisited for variable-source runoff areas, *J. Irrig. Drain. Eng.*, 121(3), 234–238.
- Tang, Q., T. Oki, S. Kanae, and H. Hu (2007), The influence of precipitation variability and partial irrigation within grid cells on a hydrological simulation, *J. Hydrometeorol.*, 8(3), 499–512.
- Tedela, N., S. McCutcheon, T. Rasmussen, and W. Tollner (2008), Evaluation and improvements of the curve number method of hydrological analysis on selected forested watersheds of Georgia, Report as of FY2007 for 2007GA143B, Ga. Water Resour. Inst. Report, Atlanta, Ga.
- Tedela, N. H., S. C. McCutcheon, T. C. Rasmussen, R. H. Hawkins, W. T. Swank, J. L. Campbell, M. B. Adams, C. R. Jackson, and E. W. Tollner (2011), Runoff curve numbers for 10 small forested watersheds in the mountains of the eastern United States, *J. Hydrol. Eng.*, 17, 1188–1198.

- Teuling, A. J., and P. A. Troch (2005), Improved understanding of soil moisture variability dynamics, *Geophys. Res. Lett.*, *32*, L05404, doi:10.1029/2004GL021935.
- Thomas, G., and A. Henderson-Sellers (1991), An evaluation of proposed representations of subgrid hydrologic processes in climate models, *J. Clim.*, *4*(9), 898–910.
- Tromp-van Meerveld, H., and J. McDonnell (2006a), Threshold relations in subsurface stormflow: 1. A 147-storm analysis of the Panola hillslope, *Water Resour. Res.*, *42*, W02410, doi:10.1029/2004WR003778.
- Tromp-van Meerveld, H., and J. McDonnell (2006b), Threshold relations in subsurface stormflow: 2. The fill and spill hypothesis, *Water Resour. Res.*, *42*, W02411, doi:10.1029/2004WR003800.
- USDA National Resources Conservation Service (2004), *National Engineering Handbook: Part 630—Hydrology*, U.S. Dep. of Agric. Nat. Resour. Conserv. Serv., Washington, D. C.
- Watson, K., and R. Luxmoore (1986), Estimating macroporosity in a forest watershed by use of a tension infiltrometer, *Soil Sci. Soc. Am. J.*, *50*(3), 578–582.
- Western, A. W., R. B. Grayson, G. Blöschl, G. R. Willgoose, and T. A. McMahon (1999), Observed spatial organization of soil moisture and its relation to terrain indices, *Water Resour. Res.*, *35*(3), 797–810.
- Western, A. W., S.-L. Zhou, R. B. Grayson, T. A. McMahon, G. Blöschl, and D. J. Wilson (2004), Spatial correlation of soil moisture in small catchments and its relationship to dominant spatial hydrological processes, *J. Hydrol.*, *286*(1), 113–134.
- Wigmosta, M. S., L. W. Vail, and D. P. Lettenmaier (1994), A distributed hydrology-vegetation model for complex terrain, *Water Resour. Res.*, *30*(6), 1665–1679.
- Woodward, D. E., R. Hawkins, A. Hjelmfelt, J. Van Mullem, and Q. Quan (2002), Curve number method: Origins, applications, and limitations, paper presented at US Geological Survey Advisory Committee on Water Information—Second Federal Interagency Hydrologic Modeling Conference, July, US Geological Survey Advisory Committee on Water Information Second Federal Interagency Hydrologic Modeling Conference, Las Vegas, Nev.
- Yeakley, J., W. Swank, L. Swift, G. Hornberger, and H. Shugart (1998), Soil moisture gradients and controls on a southern Appalachian hillslope from drought through recharge, *Hydrol. Earth Syst. Sci.*, *2*(1), 41–49.
- Yu, B. (1998), Theoretical justification of SCS method for runoff estimation, *J. Irrig. Drain. Eng.*, *124*(6), 306–310.
- Yuan, Y., J. Mitchell, M. Hirschi, and R. Cooke (2001), Modified SCS curve number method for predicting subsurface drainage flow, *Trans. ASAE*, *44*(6), 1673–1682.